IEEE Access
Multidisciplinary | Rapid Review | Open Access Journal

Received 28 October 2022, accepted 26 November 2022, date of publication 28 November 2022, date of current version 8 December 2022.

Digital Object Identifier 10.1109/ACCESS.2022.3225450

RESEARCH ARTICLE

A Simple Structure Dual-Band Dual-Circularly Polarized Antenna With Controlled Frequency Ratio

XIAN JING LIN[1], (Member, IEEE), ZHEN HUA WU[1], SHAN JIN WANG[1], ZENG PEI ZHONG[2], (Member, IEEE), YING XIN LAI[2], (Member, IEEE), AND YAO ZHANG[2], (Member, IEEE)

[1]School of Electronic Engineering and Intelligence, Dongguan University of Technology, Dongguan 523808, China
[2]Institute of Electromagnetics and Acoustics, Xiamen University, Xiamen 361005, China

Corresponding author: Yao Zhang (zhangsantu@xmu.edu.cn)

This work was supported in part by the Basic and Applied Basic Research Foundation of Guangdong Province under Grant 2020A1515110217, in part by the National Natural Science Foundation of China under Grant 62001407 and Grant 61471122, in part by the Open Program from State Key Laboratory of Millimeter Waves under Grant K202203, in part by the Guangdong Provincial Key Laboratory of Millimeter-Wave and Terahertz under Grant 2019B030301002KF2104, in part by Dongguan Sci-tech Special Commissioner Project under Grant 20201800500182, and in part by the Fundamental Research Funds for the Central Universities under Grant 20720210086.

ABSTRACT This paper proposes a dual-band dual-circularly polarized (CP) aperture-coupled patch antenna with controlled frequency ratio. By simply etching a modified S-shaped slot at the central of a circular patch, dual-band dual-CP operation is realized. In addition, the frequency ratio of the two CP bands can be controlled by optimizing the length parameters of the S-shaped slot arms. As a result, the frequency ratio can be tuned from 1.12 to 1.46 according to different requirements. For demonstration, the circularly polarized patch antenna operating at 3.42 and 3.85 GHz is manufactured and tested. The measured 3-dB axial-ratio (AR) bandwidth is 1.1% and 2.3% for the right-hand circular polarization (RHCP) and left-hand circular polarization (LHCP), respectively. The measured gains at the lower and upper bands are 9.4 and 9.8 dBic, respectively.

INDEX TERMS Circularly polarized, dual-band, patch antenna, slot coupled, controlled frequency ratio.

I. INTRODUCTION

Circularly polarized (CP) antennas have received considerable attention since they can not only alleviate multipath propagation affects and decrease polarization mismatch loss, but also suppress the Faraday effects produced by the ionosphere. Moreover, circularly polarized antennas with no need for polarization alignment, are widely used in modern wireless communication. Dual-/multi-band antennas are often employed in global navigation satellite system to ensure the accuracy of the satellite positioning. Dual-band dual-sense CP antennas are typically designed in two bands as transmitting and receiving channels to strengthen the channels isolation. For example, in the satellite communication system, the RF transmitter is required to work with LHCP operation in a lower band frequency while the RF receiver with RHCP operation in a higher frequency band.

In recent years, several dual-band CP antennas with superior performance have been presented [1], [2], [3]. However, they featured only a single RHCP or LHCP function. To realize dual-band dual-sense CP operation, two disparate radiating patches operating at inverse sense were directly connected by the feeding network in [4] and [5]. Similarly, same-layer parasitic patches [6], [7], [8], [9] and multi-layer stacked patches [10], [11], [12], [13], [14] were used to produce dual-band and dual-sense CP performances. Since independent patch radiators were employed, it's possible to control the frequency ratio of the CP bands. For example, in [14], two different size circular ring patches on different layers were excited by a dual-band

The associate editor coordinating the review of this manuscript and approving it for publication was Bilal Khawaja.

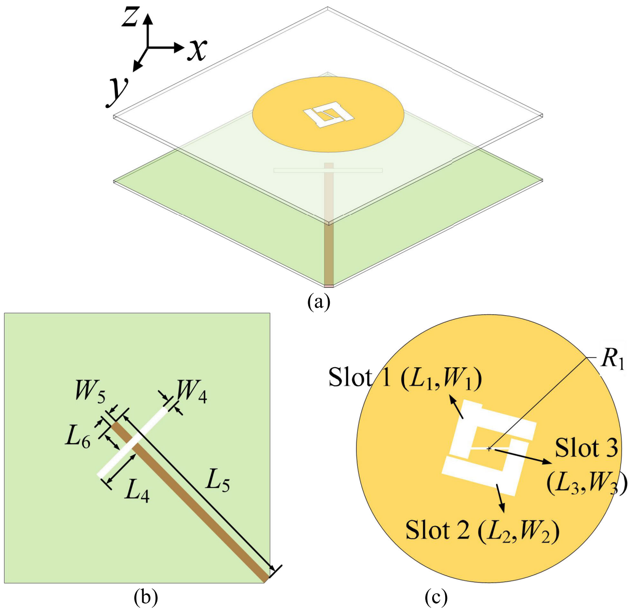

FIGURE 1. Configuration of the proposed dual-band dual-CP patch antenna, (a) 3-D view, (b) bottom view and (c) top view ($L_1 = 6.5$, $L_2 = 6.75$, $L_3 = 4.4$, $L_4 = 25$, $L_5 = 74.5$, $L_6 = 3.8$, $W_1 = W_2 = W_5 = 2.2$, $W_3 = 0.25$, $W_4 = 1.8$, all in mm).

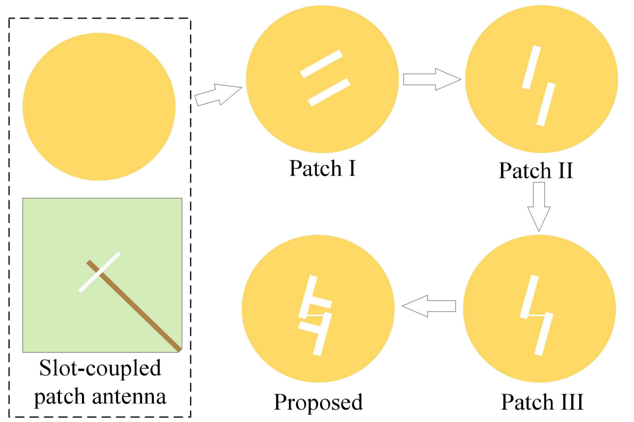

FIGURE 2. Design procedure of the proposed antenna.

phase shifter. But these methods will take considerable space and increase the complexity of the structure. A preferable option to solve this dilemma is to use slot antenna [15], [16]. Wideband and dual-sense performance can be realized by such simple slot antenna structures. However, the main disadvantage for this kind antenna is the large back-side radiation. To improve the antenna directivity, a patch antenna fed by a dual-coupled line [17] has been proposed. Dual-band dual-CP, low backside radiation and simple structure have been successfully realized. Since only one patch is employed, it is challenging to independently control the frequencies of the two CP bands.

Against this background, this paper presents a new patch antenna with a modified S-shaped slot. This slot generates the dual-band dual-CP response and the frequency of each CP band can be independently controlled by varying corresponding slot arms. Compared to the existing dual-band dual-CP antenna, the proposed antenna can realize the two CP bands independently controlled with a single radiator. The antenna is fabricated and the measured results show that it simultaneously realizes a simple structure, independent frequency control of the dual-CP band and high gain. This paper is organized as follows. The dual-band and dual-CP generation mechanism of the antenna is described in detail in Section II, a prototype with simulation and measurement results are reported in Section III. Finally, the conclusion is given in Section IV.

II. ANTENNA DESIGN

A. ANTENNA CONFIGURATION

The geometry of the proposed antenna is illustrated in Fig. 1. The antenna consists of two substrates with relative permittivity 2.55, loss tangent 0.0029 and thickness 0.8 mm. A circular patch with a modified S-shaped slot is printed on the top surface of the upper substrate. The traditional aperture-coupled feeding structure which is composed of a microstrip feeding line and a slot is used. They are printed on the bottom and top surface of the lower substrate, respectively. The input signal transmits through the microstrip line to the slot and then coupled to the patch radiator. The air gap between the two substrates is 4.2 mm.

The modified S-shaped slot is composed of two parallel arranged rectangular slots rotated 15° from the *y*-axis and a rectangular slot connecting them in the center. The arrangement of the S-shaped slot can introduce a perturbation to excite two orthogonal modes with a 90° phase-shift for CP performance. And the dual-band operation can be also generated. Moreover, we introduce another two parallel arranged rectangular slots rotated 15° from the *x*-axis to freely control the frequencies of the two CP operating bands. As shown in Fig. 1, the 15° *y*-axis rotated parallel arranged rectangular slots, the 15° *x*-axis rotated parallel arranged rectangular slots, and the center rectangular slot are denoted as Slot 1, Slot 2 and Slot 3, respectively.

B. DESIGN PROCEDURE

To illustrate the working principle of the proposed antenna, the evolution of the antenna is shown in Fig. 2. The proposed antenna originates from a traditional slot-coupled patch antenna. The patch radiator here is selected to be a circular one rather than a rectangular one. Apparently, this antenna is linear-polarized (LP). Firstly, etch two parallel arranged rectangular slots rotated 45° from the *y*-axis on the patch radiator and Patch I is realized. Secondly, rotate these two rectangular slots 30° counter-clockwise to obtain Patch II. This means the two parallel arranged rectangular slots of Patch II is 15° rotated from the *y*-axis. This rotation introduces a perturbation for the two orthogonal modes and then elliptical polarized operation is achieved. Thirdly, introduce an extra rectangular slot to connect the two parallel slots and the Patch III is realized. This rectangular slot is very essential for dual-sense CP operation.

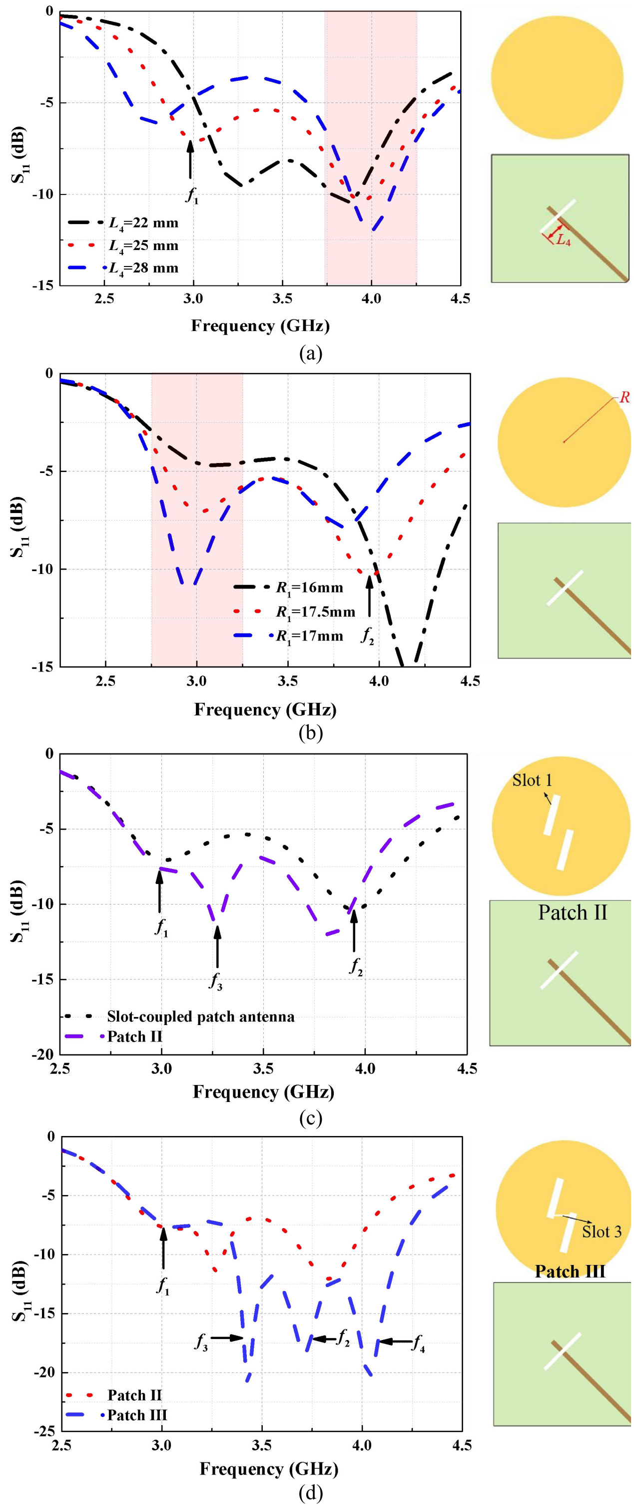

FIGURE 3. Simulated reflection coefficients of, (a) the slot-coupled antenna with L4 tuned, (b) the slot-coupled antenna with R1 tuned, (c) the slot-coupled antenna and Patch II, (d) the Patch I and Patch III.

Fig. 3 shows the simulated reflection coefficients of the slot-coupled patch antenna, Patch II and III. As is known, for the traditional side-fed patch antenna, there is only one resonant mode, resulting in limited working bandwidth. For

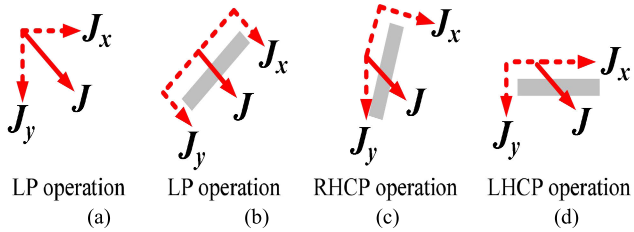

FIGURE 4. Theoretical analysis of the CP generation mechanism.

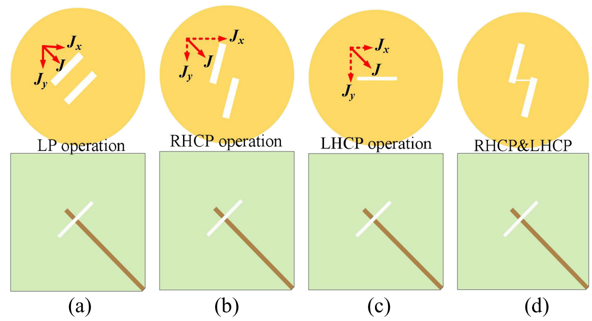

FIGURE 5. Antenna evolution of the proposed CP antenna.

bandwidth enhancement, the slot-coupling fed patch antenna is proposed by generating another resonant mode [18]. One is generated by the patch resonator and the other is generated by the coupling slot. Figs. 3(a) and (b) show the reflection coefficients of the slot-coupled fed patch antenna against the parameters L_4 and R_1. As observed, the frequencies of the two resonant modes (f_1 and f_2) can be tuned by changing the length of the patch resonator and the coupling slot. Apparently, these two resonant modes are linearly-polarized modes (f_1 and f_2).

As observed in Fig. 3(c), when two parallel arranged rectangular slots are etched on the patch, the third resonant frequency (f_3) is generated. Once another slot is employed to connect the two parallel slots, the S-shaped slot is formed and the fourth resonant frequency (f_4) is generated, as seen in Fig. 3(d). It is worth mentioning that these two resonant modes (f_3 and f_4) are circularly-polarized modes. The detailed CP generation mechanism is analyzed as below.

It is well-known that, any LP current (J) can be decomposed into two vertical LP components (J_x and J_y), as shown in Fig. 4(a). When a slot is introduced which is perpendicular to the LP current, as seen in Fig. 4(b), the current paths of J_x and J_y are the same and thus it is still the LP operation. We can change the current paths of J_x and J_y by rotating the slot direction. For example, when the slot is rotated counterclockwise with a certain angle, as seen in Fig. 4(c), the current path difference is produced between J_x and J_y. Since J_x flows ahead of J_y, it is no longer the LP operation and the main current J rotates count-clockwise, which is known as RHCP. Similarly, when the slot is rotated clockwise with a certain angle, as seen in Fig. 4(d), J_x lags behind J_y and LHCP is generated.

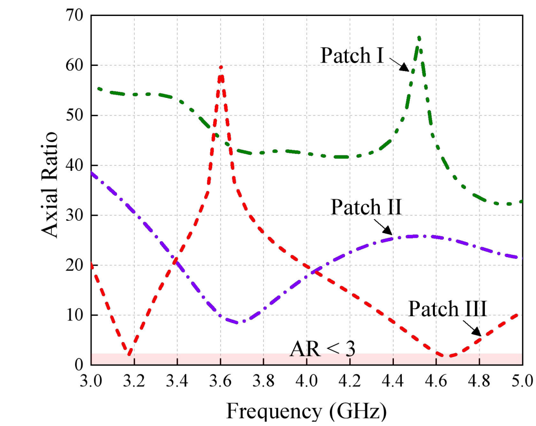

FIGURE 6. Axial ratio of the slot-coupled antenna with Patch I, II and III.

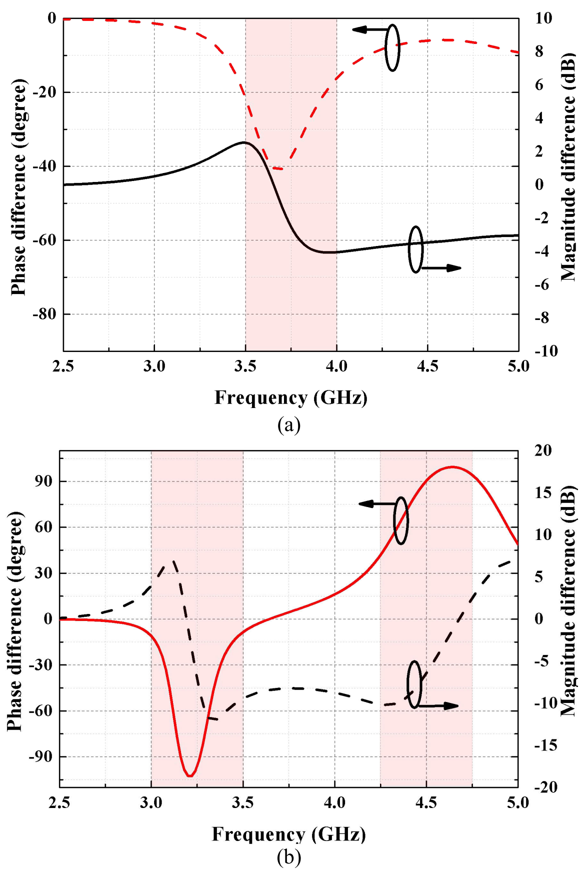

FIGURE 7. Simulated phase and magnitude difference versus frequency. (a) Patch II. (b) Patch III.

C. DESIGN GUIDELINE

Based on the above method, a design guideline of the proposed antenna with an S-shaped slot can be summarized as below:

(1) Step 1: Etch two parallel arranged rectangular slots rotated 45° from the *y*-axis on the patch radiator, as seen in Fig. 5(a). Since the slot direction and the excitation current are perpendicularly to each other, the patch (Patch I) is still the LP antenna.

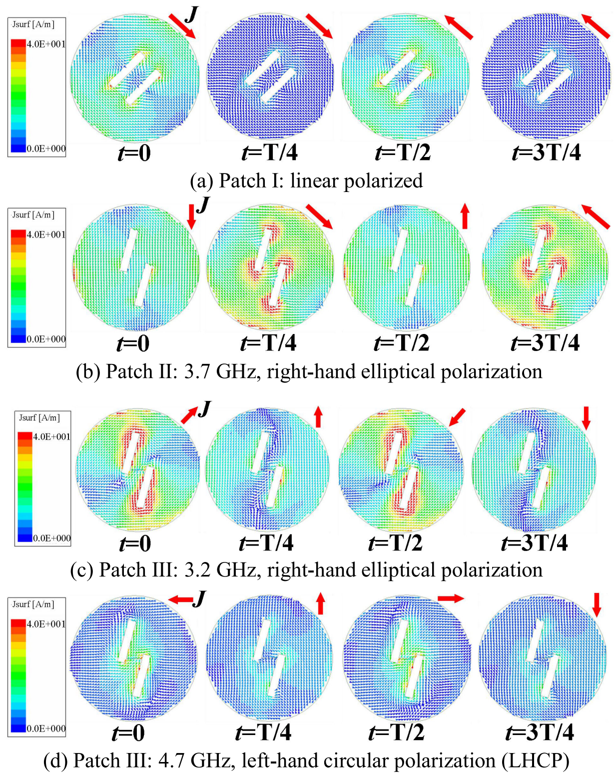

FIGURE 8. Current distributions on the (a) Patch I, (b) Patch II, (c) Patch III at 3.2 GHz and (d) Patch III at 4.7 GHz.

(2) Step 2: Rotate these two rectangular slots counterclockwise (Patch II), as shown in Fig. 5(b). Tune the slot angle to optimize its RHCP performance.

(3) Step 3: Add a horizontal slot to realize LHCP performance, as shown in Fig. 5(c).

(4) Step 4: Combine the slots together to form an S-shaped slot (Patch III), as presented in Fig. 5(d), and dual-sense CP operation can be thus realized.

(5) Step 5: Since the RHCP and LHCP performance can be optimized by controlling the parameters of the corresponding Slot 1 and Slot 3, refine each parameter such as the slot length, angle and width to obtain good impedance matching and AP performance.

Fig. 6 reveals the axial ratios (AR) of the Patch I, II and III. For the Patch I, the axial ratio is above 35 dB from 2.5-5.5 GHz. For the Patch II, this value is decreased to 10 dB at about 3.7 GHz. Furthermore, for the Patch III, the AR reduces to about 3 dB at about 3.2 and 4.7 GHz. Fig. 7 describes the phase and magnitude difference versus frequency of the Patch II and III. For the Patch II at 3.7 GHz, the magnitude difference is 0 dB and the phase difference is about 40 degree. While for the Patch III, the magnitude and phase difference is 0 dB and 100 degree at 3.2 GHz, and 0 dB and 98 degree at 4.7 GHz. The above results verified that the S-shaped slot can obtain dual band and dual sense.

To further reveal the antenna working mechanism, the vector current distributions orientated at $t = 0$, T/4, T/2, and 3T/4 of the three antennas are shown in Fig. 8. For Patch I seen in Fig. 8(a), it is apparently a −45° linear polarized (LP)

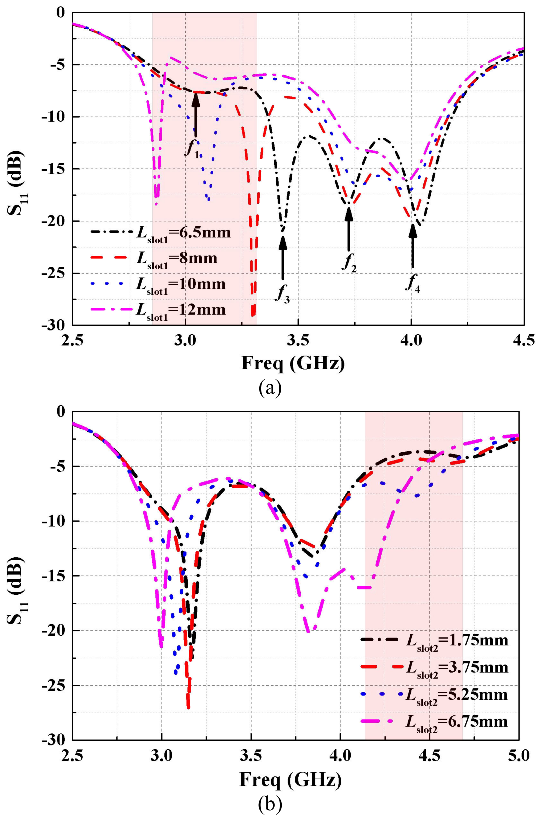

FIGURE 9. **Simulated reflection coefficients of the proposed antenna against the parameters (a) L_{slot1} and (b) L_{slot2}.**

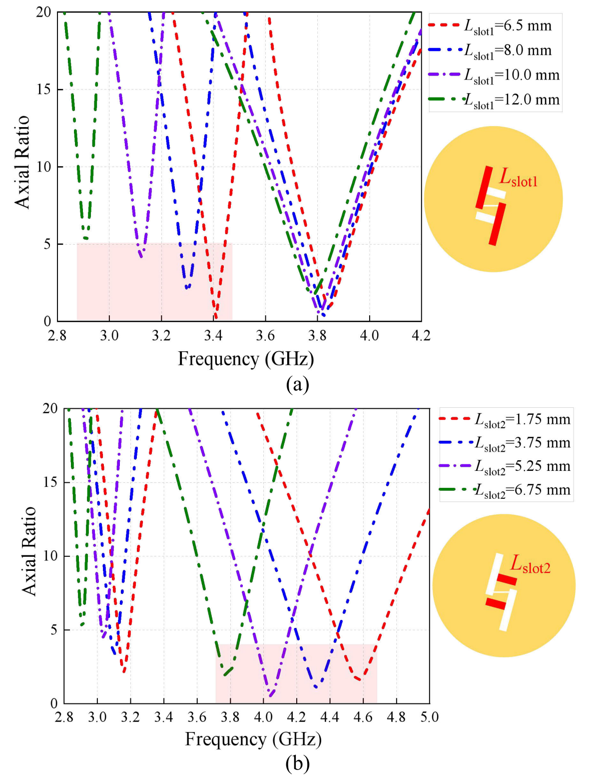

FIGURE 10. **Axial ratio of the proposed antenna against the parameters (a) L_{slot1} and (b) L_{slot2}.**

patch antenna. However, for Patch II, it is no longer a LP antenna. The currents at t = 0, T/4, T/2, and 3T/4 rotate counter clockwise as shown in Fig. 8(b), indicating that the right-hand elliptical polarization is realized at 3.7 GHz. With regard to Patch III, the right-hand elliptical polarization and left-hand circular polarization (LHCP) is realized at 3.2 GHz and 4.7 GHz, respectively. Above results verify the analysis.

Although the Patch III achieves dual-band dual-sense operation, the axial ratios of these two working bands are not satisfactory. Therefore, the proposed dual-band dual-CP antenna is developed by adding another two parallel arranged rectangular slots rotated 15° from the x-axis. With these two slots, the frequencies of the two CP operating bands can be freely controlled, which is detailed presented in the following section.

D. FLEXIBLE CONTROL OF THE TWO CP BANDS

It's worth mentioning that as observed in Fig. 8(c) and (d), the current path at 3.2 GHz mainly flows along the Slot 1 (the 15° y-axis rotated parallel arranged rectangular slots). At 4.7 GHz, the currents around the Slot 1 are not strong and part of them concentrate on the Slot 3 (the center rectangular slot). These results indicate that the Slot 1 has large effect on the performance of the lower frequency band 3.2 GHz. Since the Slot 3 affects the performance of upper-band 4.7 GHz, we thus deliberately introduce the Slot 2 shown in Fig. 1 to extend the current path of 4.7 GHz.

For demonstration, the reflection coefficients and the axial ratios of the proposed antenna against the length parameters L_{slot1} and L_{slot2} are illustrated in Fig. 9 and Fig. 10, respectively. As the length of the Slot 1 increases from 6.5 mm to 12.0 mm, the lower-band resonating frequency and the AR frequency decreases from about 3.4 GHz to 2.9 GHz with the upper-band resonating frequency and the AR frequency almost unchanged. Similar phenomenon is observed that as the length of the Slot 2 increases from 1.75 mm to 6.75 mm, the upper-band AR frequency decreases from about 4.6 GHz to 3.8 GHz. It should be mentioned that although the resonating frequency and the AR band frequencies are changed with different L_{slot2}, the length of the Slot 2 has larger effect on the upper-band one. Above results agree well with the analysis. By optimizing the parameters of the Slot 1 and Slot 2, the frequency ratio of the two CP bands can be freely controlled.

In this work, the parameters L_{slot1} and L_{slot2} are finally selected to be 6.5 and 6.75 mm for both good impedance matching and AR values. Fig. 11 shows the current distribution on the proposed patch at the lower and upper-band frequencies. As seen, standard RHCP and LHCP operations are achieved as expected.

III. ANTENNA IMPLEMENTATION

Based on the above-mentioned design method, the proposed dual-band dual-circularly polarized patch antenna is fabricated and measured, with the results shown in Fig. 12. In this

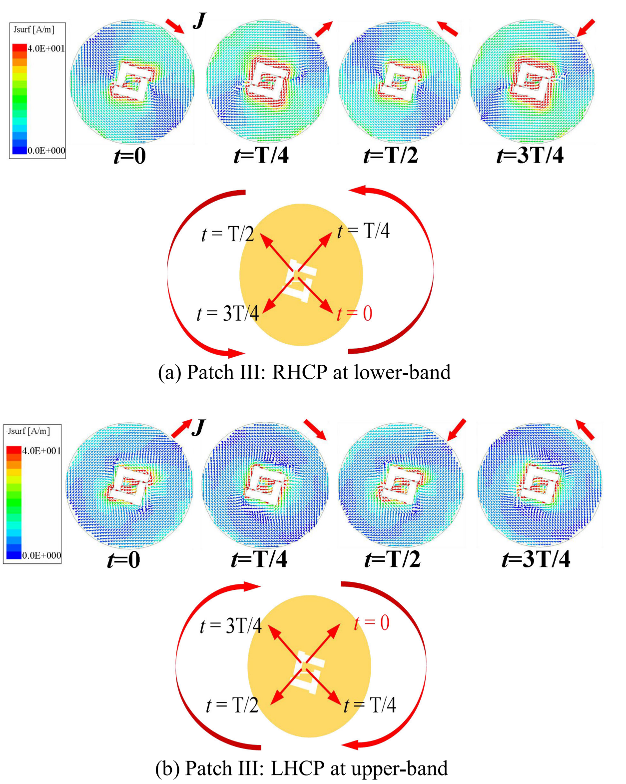

(a) Patch III: RHCP at lower-band

(b) Patch III: LHCP at upper-band

FIGURE 11. **Current distribution on the proposed patch at (a) lower-band and (b) upper-band.**

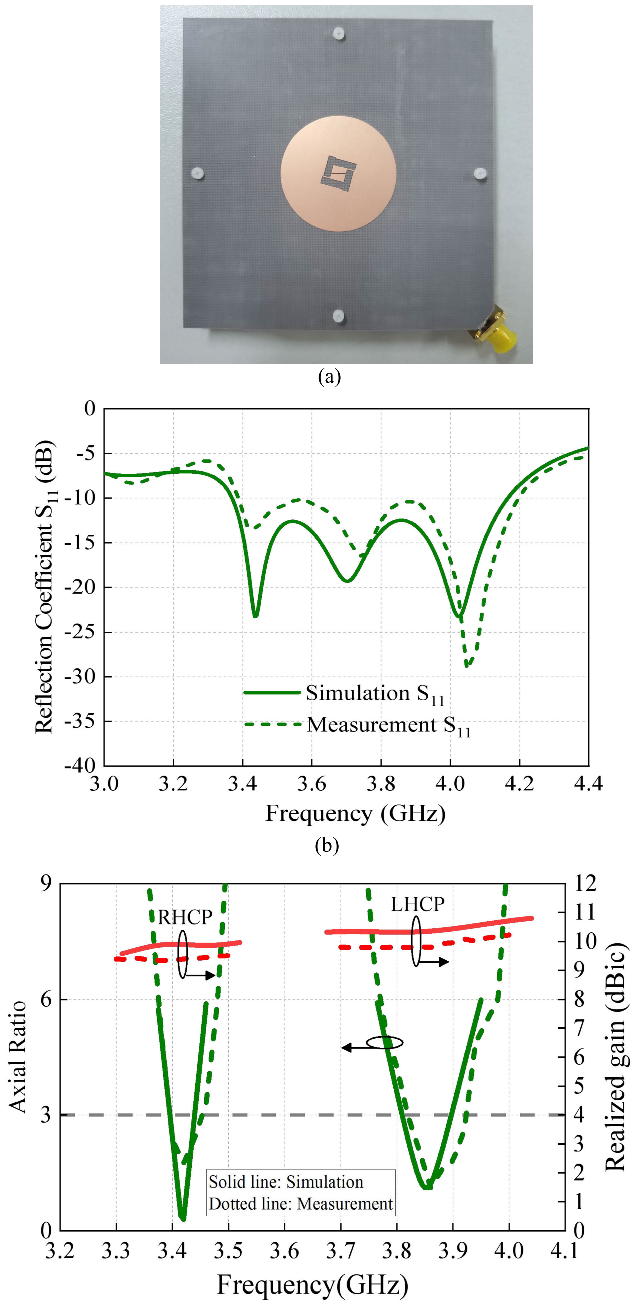

(a)

(b)

(c)

FIGURE 12. **Results of the proposed antenna including (a) antenna prototype, (b) reflection coefficient S_{11} and (c) gain and AR.**

work, the antenna CP frequency bands are set to be 3.42 and 3.85 GHz as an example to verify the design method. In fact, the two CP bands can be controlled to the desired frequencies by optimizing the length and angle of the Slot 1 and Slot 3. It should be mentioned that according to the simulation results, the frequency ratio of this design can be easily tuned from 1.12 to 1.46 with both satisfactory impedance matching and AR performance.

Fig. 12(a) shows the fabrication prototype and the results are potted in Figs. 12(b) and (c). The measurement results agree well with simulation ones. The difference between the measured and simulated results is mainly due to the fabrication tolerance and other measurement imperfections. The measurement was accomplished by Agilent 5071C network analyzer and Satimo Starlab system. The measured impedance bandwidth is 21.22 % (3.37-4.17 GHz). And the measured 3-dB AR bandwidths at the lower and higher bands are 1.16 % (3.40-3.44 GHz), 2.33 % (3.81-3.90 GHz), respectively. The measured average gains are 9.4 and 9.8 dBic. Fig. 13 depicts the simulated and measured RHCP and LHCP radiation patterns in the *xoz* and *yoz* plane at 3.42 GHz and 3.85 GHz. Directive radiation patterns with low cross-polarization levels are obtained.

To address the advantages of the proposed work, some latest researches are compared and the results are tabulated in Table 1. The designs in [1], [2], and [3] realized single-polarized response. In [4], [9], and [13], disparate patches were employed to realize dual-CP function and wider AR bandwidth. However, the dual-band dual-sense CP antenna realization method is not attractive by using two disparate stacked radiating patches operating at inverse sense, resulting in considerable antenna space and increased the complexity. In [15], wideband CP performance was realized by a simple slot antenna structure. However, the backside radiation is relatively high and the two CP bands of the antenna cannot be controlled. A planar patch antenna was proposed in [17] but the CP bandwidths are limited. It's worth mentioning that all the above dual-band dual-CP antennas cannot realize the frequency control of the CP bands. In addition, compared to

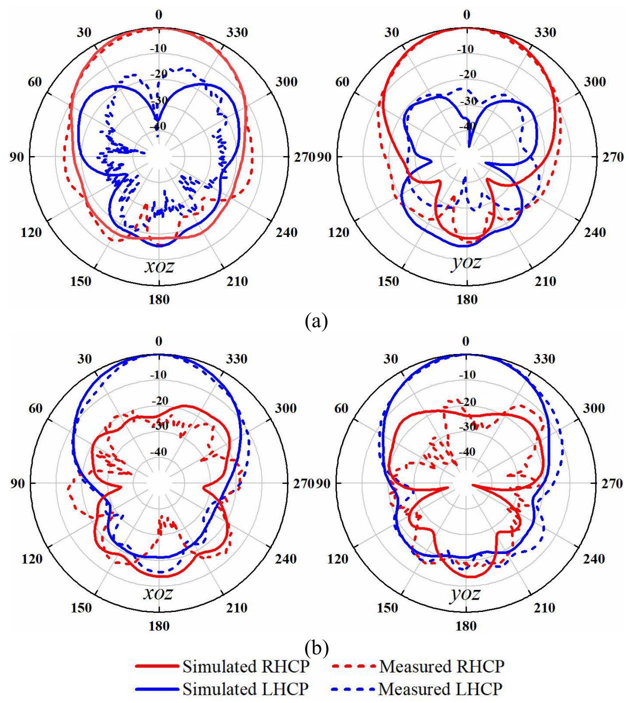

FIGURE 13. Radiation patterns of antenna at (a) 3.42 GHz (b) 3.85 GHz.

TABLE 1. Performance comparison.

Ref.	Realization	AR bandwidth	Polar.	Gain (dBic)	Freq. control
[1]	Patch + AMC reflector	5.25% /2%	Single	2.91, /6.25	No
[2]	Ring patch	1.5% /1%	Single	3.68, /3.31	No
[3]	Slotted patch	6.9% /0.6%	Single	5.0 /5.0	Yes
[4]	Disparate patch array	13.3% /7.4%	Dual	13.2 /13.9	N. A.
[9]	Patch array + parasitic resonators	0.9% /0.3%	Dual	11.7 /11.8	No
[13]	Dual-layer stacked patches	1.5% /1.1%	Dual	3.3 /4.2	No
[15]	Slot antenna	32.14% /31.49%	Dual	3.36 /4.19	No
[17]	Patch + coupled line	0.33% /0.72%	Dual	5.3 /5.7	No
This work	**Patch**	**1.16% /2.33%**	**Dual**	9.4 /9.8	**Yes**

these designs ([3] and [8] employed a 2×2 array structure), the gain (9.4 and 9.8 dBic) of the proposed design was the highest one. In all, compared to the above designs, the proposed work realize a very simple structure and the dual-band dual-sense CP operation. Moreover, the frequencies of the two CP bands can be controlled and optimized.

IV. CONCLUSION

A simple dual-band dual-sense antenna with controllable frequency ratio has been proposed in this letter. By introducing a modified S-shaped slot, dual-dual dual-CP operation has been obtained. The measured 3-dB AR bandwidth of the dual-CP is 1.1% (3.42 GHz) and 2.3% (3.85 GHz), respectively. And the center frequency of each CP band can be independently controlled by changing the length of the S-slot arms. The design procedure and working principle of this antenna have been revealed in detail. Satisfactory measurement results have been obtained as expected. The proposed design method is useful for Antennas & Propagations community.

REFERENCES

[1] S. Sarkar and B. Gupta, "A dual-band circularly polarized antenna with a dual-band AMC reflector for RFID readers," *IEEE Antennas Wireless Propag. Lett.*, vol. 19, no. 5, pp. 796–800, May 2020.

[2] C. Sahana, M. Nirmala, and M. Jayakumar, "Dual-band circularly polarized annular ring patch antenna for GPS-aided GEO-augmented navigation receivers," *IEEE Antennas Wireless Propag. Lett.*, vol. 21, no. 9, pp. 1737–1741, Sep. 2022.

[3] Nasimuddin, Z. N. Chen, and X. Qing, "Dual-band circularly polarized *S*-shaped slotted patch antenna with a small frequency-ratio," *IEEE Trans. Antennas Propag.*, vol. 58, no. 6, pp. 2112–2115, Jun. 2010.

[4] S. Ye, J. Geng, X. Liang, Y. J. Guo, and R. Jin, "A compact dual-band orthogonal circularly polarized antenna array with disparate elements," *IEEE Trans. Antennas Propag.*, vol. 63, no. 4, pp. 1359–1364, Apr. 2015.

[5] J.-D. Zhang, W. Wu, and D.-G. Fang, "Dual-band and dual-circularly polarized shared-aperture array antennas with single-layer substrate," *IEEE Trans. Antennas Propag.*, vol. 64, no. 1, pp. 109–116, Jan. 2016.

[6] C. Deng, Y. Li, Z. Zhang, G. Pan, and Z. Feng, "Dual-band circularly polarized rotated patch antenna with a parasitic circular patch loading," *IEEE Antennas Wireless Propag. Lett.*, vol. 12, pp. 492–495, 2013.

[7] Z.-X. Liang, D.-C. Yang, X.-C. Wei, and E.-P. Li, "Dual-band dual circularly polarized microstrip antenna with two eccentric rings and an arc-shaped conducting strip," *IEEE Antennas Wireless Propag. Lett.*, vol. 15, pp. 834–837, 2016.

[8] X. L. Bao and M. J. Ammann, "Dual-frequency circularly-polarized patch antenna with compact size and small frequency ratio," *IEEE Trans. Antennas Propag.*, vol. 55, no. 7, pp. 2104–2107, Jul. 2007.

[9] Q.-S. Wu, X. Zhang, L. Zhu, J. Wang, G. Zhang, and C.-B. Guo, "A single-layer dual-band dual-sense circularly polarized patch antenna array with small frequency ratio," *IEEE Trans. Antennas Propag.*, vol. 70, no. 4, pp. 2668–2675, Apr. 2022.

[10] Y. Liu, Z. Yue, Y. Jia, Y. Xu, and Q. Xue, "Dual-band dual-circularly polarized antenna array with printed ridge gap waveguide," *IEEE Trans. Antennas Propag.*, vol. 69, no. 8, pp. 5118–5123, Aug. 2021.

[11] K. Ding, Y. Wu, K.-H. Wen, D.-L. Wu, and J.-F. Li, "A stacked patch antenna with broadband circular polarization and flat gains," *IEEE Access*, vol. 9, pp. 30275–30282, 2021.

[12] S. Wang, L. Zhu, and W. Wu, "3-D printed inhomogeneous substrate and superstrate for application in dual-band and dual-CP stacked patch antenna," *IEEE Trans. Antennas Propag.*, vol. 66, no. 5, pp. 2236–2244, May 2018.

[13] H. Yang, Y. Fan, and X. Liu, "A compact dual-band stacked patch antenna with dual circular polarizations for BeiDou navigation satellite systems," *IEEE Antennas Wireless Propag. Lett.*, vol. 18, no. 7, pp. 1472–1476, Jul. 2019.

[14] W. Wang, C. Chen, S. Wang, and W. Wu, "Switchable dual-band dual-sense circularly polarized patch antenna implemented by dual-band phase shifter of ±90°," *IEEE Trans. Antennas Propag.*, vol. 69, no. 10, pp. 6912–6917, Oct. 2021.

[15] W.-C. Weng, J.-Y. Sze, and C.-F. Chen, "A dual-broadband circularly polarized slot antenna for WLAN applications," *IEEE Trans. Antennas Propag.*, vol. 62, no. 5, pp. 2837–2841, May 2014.

[16] X. Bao and M. J. Ammann, "Dual-frequency dual-sense circularly-polarized slot antenna fed by microstrip line," *IEEE Trans. Antennas Propag.*, vol. 56, no. 3, pp. 645–649, Mar. 2008.

[17] Z. P. Zhao, F. Liu, J. Ren, Y. Liu, and Y. Z. Yin, "Dual-sense circularly polarized antenna with a dual-coupled line," *IEEE Antennas Wireless Propag. Lett.*, vol. 19, no. 8, pp. 1145–1149, Aug. 2020.

[18] Q. Rao and R. H. Johnston, "Modified aperture coupled microstrip antenna," *IEEE Trans. Antennas Propag.*, vol. 52, no. 12, pp. 3397–3401, Dec. 2004.

XIAN JING LIN (Member, IEEE) was born in Hunan, China. She received the Ph.D. degree in electromagnetic and microwave technology from the South China University of Technology, in 2017. She is currently with the Dongguan University of Technology, School of electronic engineering and intelligence, as a Lecturer. Her research interests include filtering duplex antenna integration, microwave circuit and massive MIMO antennas. She serves as a Reviewer for several journals, including the IEEE Antennas and Wireless Propagation Letters, and *International Journal of Antennas and Propagation*.

ZHEN HUA WU was born in Guangdong, China, in 2000. He is currently pursuing the B.S. degree in communication engineering from the Dongguan University of Technology, Dongguan, China. His current research interest includes on multi-frequency circularly polarized antennas.

SHAN JIN WANG was born in Jiangxi, China. He received the B.S. degree in physics from the East China Institute of Technology, Jiangxi, in 1986, the M.S. degree in physics from South China Normal University, Guangzhou, China, in 1992, and the Ph.D. degree in physical electronics from Southeast University, Nanjing, China, in 2002. He is currently a Professor with the School of Electronic Engineering and Intelligence, Dongguan University of Technology. His current research interests include microwave and radio frequency circuit design, antenna miniaturization design, and radio frequency identification theory and application.

ZENG PEI ZHONG (Member, IEEE) was born in Puning, China. He received the B.E. degree in applied physics and the Ph.D. degree in information and communication engineering from Shenzhen University, Shenzhen, China, in 2016 and 2021, respectively. He is currently a Lecturer with the Dongguan University of Technology. His current research interests include circularly-polarized antennas and functional planar antennas.

YING XIN LAI (Member, IEEE) received the B.S. and Ph.D. degrees from Southwest Jiaotong University (SWJTU), Chengdu, China, in July 2003 and December 2008, respectively.

He is currently an Associate Professor with the School of Electronic Engineering and Intelligentization, Dongguan University of Technology (DGUT), Dongguan, China. His research interests include high-power microwave sources, antennas, millimeter passive devices, and microwave-photonic sensors.

YAO ZHANG (Member, IEEE) received the Ph.D. degree in electronics and information engineering from the School of Electronic and Information Engineering, South China University of Technology, Guangzhou, China, in 2019.

In 2014, he joined the City University of Hong Kong Shenzhen Research Institute, Shenzhen, China, as a Researcher. In September 2018, he joined the Department of Electrical and Computer Engineering, Duke University, Durham, NC, USA, as a Visiting Scholar, under the financial support from China Scholarship Council. He is currently an Assistant Professor with the School of Electronic Science and Engineering, Institute of Electromagnetics and Acoustics, Xiamen University. He has authored or coauthored more than 40 internationally referred journal articles. His current research interests include microwave and millimeter-wave circuits, massive multiple-input-multiple-output (MIMO) antennas, base-station array antennas, antenna-in-package (AIP), and integration designs of filter and antenna. He was a recipient of the Nominee Award of 2020 Excellent Doctoral Dissertation of China Education Society of Electronics (CESE), the Best Student Paper Award at the IEEE 5th Asia-Pacific Conference on Antenna and Propagation (APCAP), the National Scholarship for Graduate Students (2015, 2016, and 2017), the Outstanding Doctoral Dissertation Innovation Funds from South China University of Technology (2015, 2016, and 2017). He has served as a technical program committee member, an invited speaker, and the session organizer/chair for a number of conferences. He also serves as a Reviewer for several international journals including IEEE Transactions on Antennas and Propagation, IEEE Antennas and Wireless Propagation Letters and IEEE Access.